

Comparison of in vivo 3D flow characteristics to realistic in vitro models with flexible and rigid vessel wall

Ramona Lorenz¹, Michael Markl², Stephan Berner¹, Christoph Müller¹, and Bernd Jung¹

¹Dept. of Radiology, Medical Physics, University Medical Center Freiburg, Freiburg, Germany, ²Dept. of Radiology and Biomedical Engineering, Northwestern University, Chicago, Illinois, United States

Purpose: For a better diagnosis and treatment of cardiovascular diseases it is necessary to investigate the cause and relationship between morphological and functional changes of the heart and vessels. In addition to longitudinal *in vivo* studies, realistic in-vitro model systems of vascular systems such as the aorta have the potential helping to understand the link between progression of vascular diseases (such as aortic coarctation or aneurysms) and their association with complex hemodynamic alterations. Recently, realistic vascular *in vitro* phantoms in combination with a pulsatile flow circuit and 4D MRI flow measurements were employed to simulate realistic *in vivo* hemodynamics [1,2]. However, previous vessel models consisted of a rigid material and it is unclear how the absence of vessel wall compliance influenced the resulting 3D blood flow inside the model system. Thus, the aim of this study was to perform *in vitro* model experiments using realistic vessel models of the thoracic aorta made with a flexible material to investigate the impact of different wall thicknesses (simulating different levels of elasticity) on hemodynamics. Results were compared to *in vitro* models with rigid vessel walls and to *in vivo* 3D flow characteristics in the subject's aorta used to generate the *in vitro* model.

Methods: Figure 1 illustrates the setup of the MR-compatible flow cycle for the *in vitro* models with integrated pressure control unit in the MR-scanner and the pump control unit (MEDOS Medizintechnik AG, Germany) in the console room. The *in vitro* models represent a one-to-one replica of a normal aorta and were generated by rapid prototyping. Different wall elasticity was achieved by different wall thickness (4-7 mm). The experiments set up permits physiological in-flow conditions by a MR-compatible pneumatically driven ventricular assist device (VAD), a pump chamber including valve regulated in and out flow. The VAD was attached to the AAo of the *in vitro* models. The resulting flow data were compared to *in vitro* models with rigid vessel wall and to *in vivo* 3D flow characteristics. VAD pump performance was improved for optimal filling and emptying of the pump chamber. To imitate the physiological properties of blood, blood mimicking fluid was used (viscosity: $4.8 \cdot 10^{-3}$ Pa·s; density: 1119.7 kg/m^3 at 20°C); contrast agent was added to increase SNR. All experiments were performed on a 3T MR system (TRIO, Siemens, Germany) using a time resolved phase contrast MRI pulse sequence with three-directional velocity encoding [3]. 3D visualization (EnSight, CEI, NC, USA) was employed to compare *in vivo* and *in vitro* 3D flow characteristics. A home built tool (Matlab, The Mathworks, USA) was used for lumen contour segmentation and flow velocity quantification in 8 slices distributed along the aorta (figure 2, white lines).

Results: 3D streamline visualization for the healthy subject and the *in vitro* models with different vessel wall flexibility are illustrated in figure 2. 3D blood flow acquired *in vivo* demonstrated higher velocities over the entire aorta in particular for the peak systole. These findings are confirmed by results of velocities averaged over the entire cardiac cycle $\langle v \rangle_{avg}$ and systolic peak velocities $peak(\langle v(t) \rangle)$ in figure 3 showing highest velocities for the *in vivo* data for $peak(\langle v(t) \rangle)$. For $\langle v \rangle_{avg}$ only small differences between *in vivo* and *in vitro* were observed. The *in vivo* data and the *in vitro* models showed a similar pattern of $peak(\langle v(t) \rangle)$ along the aorta. Figure 4 illustrates time-resolved courses of $\langle v(t) \rangle$, flow rate and area change due to the pulsatility in the AAo. Higher peak velocities and a shorter systole can be observed for the *in vivo* data. Minor differences (in all planes) of $\langle v(t) \rangle$ and flow rates between the model with the rigid wall and the flexible models are revealed during early systole as well as during the downslope in mid systole (see arrows). The area change between diastole and systole was between 28% (7 mm model) and 47% for the most flexible model (4 mm).

Discussion: The study shows first results for an *in vitro* model with rigid vessel walls and four *in vitro* models with different wall elasticity. The flexibility grades do not correlate to *in vivo* conditions; however, the behavior of the peak velocities along the aorta in all *in-vitro* models agrees very well with the pattern in the *in vivo* data. 3D streamline analysis revealed a distinct flow jet directed towards the inner vessel wall of the *in vitro* models with 4 mm and 5 mm vessel wall. This effect may result from a different angle of the VAD to the AAo due to manually attaching the VAD to the *in vitro* models prior to each measurement. The origin of the subtle differences of velocities and flow rates between the model with the rigid wall and the flexible models (which may arise from the interaction of the VAD valve with the flexible walls) remains to be elucidated. In conclusion, despite the pronounced area change indicating the high flexibility of the aortic models (similar to *in vivo* scenarios), only minor differences could be observed between the rigid and the flexible models. Within the limits of the model system such as the long duration of the VAD's systole (and therefore lower velocities) in comparison with the *in vivo* data, a rigid model may also be used to simulate hemodynamic changes caused by geometric alterations. However, further experiments and refinement of models are useful to approach realistic conditions as close as possible to enhance the understanding of flow characteristics observed in *in vivo* measurements using *in vitro* models.

References: [1] Canstein C, et al. MRM 2008;59(3):535-546; [2] Lorenz R, et al. MRM 2012; 67(1):258-268; [3] Markl M, et al. JMRI, 2003; 17(4):499-506.

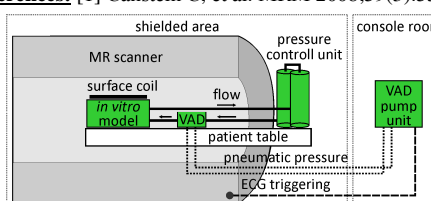


Figure 1: Set up of the pneumatically driven VAD pump system with *in vitro* model in the shielded area of the MR scanner (left) and the console room (right). The pressure control unit served as reservoir.

parameter	<i>in vivo</i>	<i>in vitro</i>	Table 1: Measurement parameters for <i>in vivo</i> data and the <i>in vitro</i> models of the aorta.
ven. [m/s]	1.5	1.5	
temp. res. [ms]	40.8	42.4	
spat. res. [mm ³]	$2.0 \times 1.7 \times 2.2$	$1.4 \times 1.4 \times 1.4$	
TR / TE [ms]	5.1 / 2.5	5.3 / 2.8	
flip angle [°]	7	40	

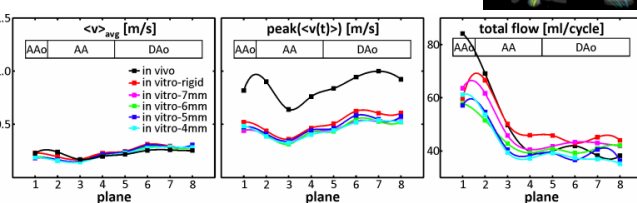


Figure 3: $\langle v \rangle_{avg}$, $peak(\langle v(t) \rangle)$ and total flow over 8 planes along the aorta of *in vivo* data and *in vitro* models with flexible vessel walls.

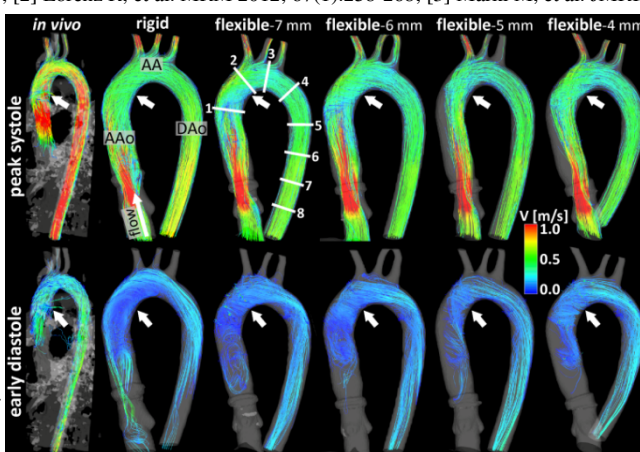


Figure 2: 3D streamlines visualization of the aorta in the healthy subject and the *in vitro* models with rigid and flexible vessel walls during peak systole and early diastole. Note the change of helical flow in the ascending aorta and the aortic arch (white arrows). The healthy subject shows the highest velocities in particular in the DAO while the *in vitro* model reveals high velocities at the inlet of the AAo. In flow during peak systole for *in vitro* models with flexible vessel wall of 5 and 4 mm is directed toward the inner vessel wall of the *in vitro* models.

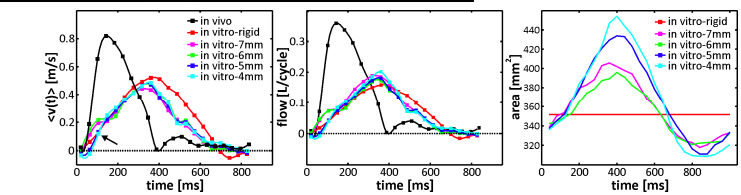


Figure 4: Time-resolved $\langle v(t) \rangle$, flow and area change in the AAo (plane 1) of *in vivo* data (vessel area not available) and *in vitro* models with different flexible walls.